Distribution of the logarithms of currents in percolating resistor networks. II. Series expansions

Joan Adler,* Amnon Aharony,† and Raphael Blumenfeld‡
School of Physics and Astronomy, Raymond and Beverly Sackler Faculty of Exact Sciences, Tel Aviv University, Tel Aviv, 69978, Israel

A. Brooks Harris§
Department of Physics, University of Pennsylvania, Philadelphia, Pennsylvania 19104

Yigal Meir**
School of Physics and Astronomy, Raymond and Beverly Sackler Faculty of Exact Sciences, Tel Aviv University, Tel Aviv, 69978, Israel

(Received 7 February 1992; revised manuscript received 16 September 1992)

We investigate the distribution of the logarithms, log$i$, of the currents in percolating resistor networks via the method of series expansions. Exact results in one dimension and expansions to thirteenth order in the bond occupation probability, p, in general dimension, for the moments of this distribution have been generated. We have studied both the moments and cumulants derived therefrom with several extrapolation procedures. The results have been compared with recent predictions for the behavior of the moments and cumulants of this distribution. An extensive comparison between exact results and series of different lengths in one dimension sheds light on many aspects of the analysis of series with logarithmic corrections. The numerical results of the series expansions in higher dimensions are generally consistent with the theoretical predictions. We confirm that the distribution of the logarithms of the currents is unifractal as a function of the logarithm of linear system size, even though the distribution of the currents is multifractal.

I. INTRODUCTION

Multifractal distributions have been the topic of much recent research. Here we study the distribution of currents in randomly diluted resistor networks at the percolation threshold. The first paper in this sequence[1] (referred to as ABH in what follows), contains a detailed review of relevant earlier work. In that paper, ABH presented a theory for the asymptotic distribution of the logarithms of the currents $[y \equiv -\ln(i^2)]$ in percolating resistor networks, with detailed predictions concerning the moments and the cumulants of this distribution.

In ABH we considered "percolating networks," i.e., randomly diluted resistor networks at the percolation threshold, $p = p_c$, where p is the concentration of conducting bonds, with unit conductance. The results of ABH concerned the multifractal distribution of currents as a function of the distance between the electrodes, L. In particular, at large L, the kth moment ($\langle y^k \rangle$) was predicted to behave as $(\ln L)^k$, with universal amplitudes, and all the corresponding cumulants ($\langle y^k \rangle_c$) were predicted to be linear in $\ln L$. Thus, the distribution of the logarithms of the currents is expected to be *unifractal* as function of $\ln L$, with the same L dependence (proportional to $\ln L$) for the ratio of any two consecutive moments (unlike these ratios for moments of the currents themselves, which require an infinite set of independent exponents).

In addition to the asymptotic behavior, ABH also found large finite-size corrections, whose relative order scales as $1/\ln L$. This means that the finite-size corrections have a much greater impact on finite simulations[2] than is the case with the usual power-law corrections. We now believe that these effects were responsible for problems in the interpretation of simulation studies[2] and series analysis (see below). It is reasonable to infer that all simulations on realistic sample sizes are strongly affected by these corrections, and therefore it is important to explore the distribution of the logarithms of the currents on percolating systems with alternative techniques. In the present paper we study the moments and cumulants of the logarithms of the currents using low concentration series expansions. Instead of treating approximately large but finite-sized samples, this technique averages *exactly* over *all* clusters having up to N bonds, where N is the order up to which the power series in the concentration p is developed. The asymptotic behavior of the average moments as p approaches p_c reflects their size dependence at large L. Experience shows[3] that relatively few terms in such series capture much of the asymptotic behavior, without severe finite-size effects.

Series expansions were previously used[4] to study susceptibilities associated with the $2q$th moment of the currents themselves, yielding the multifractal behavior of these moments for $q > q_c$ and deviations from multifractality for $q < q_c$, for a negative critical value q_c. Here we extend this approach to the study of the logarithms of the currents. Scaling theory[5] usually implies that for $p \neq p_c$ one should replace L by the pair-connectedness (percolation) correlation length $\xi_p \propto |p_c - p|^{-\nu}$. Therefore, we expect that the kth cumulant and moment will diverge near p_c as $\ln|p_c - p|$ and $|\ln|p_c - p||^k$, respectively, with correc-

tions of relative order $1/|\ln|p_c-p||$. Indeed, our results are consistent with such predictions.

Section II below explains the modifications in the relevant results of ABH required in order to make comparisons with the present series analysis. There are two major changes: First, we study the moments as a function of p, not L. Second, we impose a unit voltage rather than a unit current between the electrodes. This yields finite contributions from all the singly connected bonds, which had unit current, and therefore zero logarithm, in ABH. Particularly, this yields nontrivial results in one dimension, as outlined in Sec. IV below. The derivation of the series and the details of the methods of analysis are presented in Sec. III. Exact results as well as analysis[6-11] of series for one dimension and on the Cayley tree are given in Sec. IV, and details of the analysis for dimensions $2\le d\le 6$ are described in Sec. V. We conclude in Sec. VI with a discussion of the implications of our studies.

II. DEFINITIONS AND THEORETICAL EXPECTATIONS

Consider a dilute resistor network, so that each conductance randomly assumes the values 1 or 0 with respective probabilities p and $(1-p)$. Consider an arbitrary fixed cluster, in which a unit current is injected at a source site $\mathbf{x}$ and removed at a sink site $\mathbf{x}'$. As a result, a current of magnitude $i_b(\mathbf{x},\mathbf{x}')$ flows through the bond b on the cluster. The unnormalized $2q$th moment of these currents is defined as[1,4,12]

$$m_q(\mathbf{x},\mathbf{x}')=\sum_b i_b(\mathbf{x},\mathbf{x}')^{2q} , \tag{2.1}$$

where the sum contains only bonds with $i_b\neq 0$. ABH considered the normalized average of $m_q(\mathbf{x},\mathbf{x}')$ over all configurations of conductances,

$$M_q(\mathbf{x},\mathbf{x}')=[m_q(\mathbf{x},\mathbf{x}')]_{\rm av}/[N_{\rm BB}]_{\rm av} , \tag{2.2}$$

where $[N_{\rm BB}]_{\rm av}=[m_0]_{\rm av}$ is the average mass of the backbone (i.e., the number of current-carrying bonds) (Refs. 13 and 14) connecting the two sites $\mathbf{x}$ and $\mathbf{x}'$. For $1\ll|\mathbf{x}-\mathbf{x}'|\ll\xi_p$, one has the multifractal behavior

$$M_q(\mathbf{x},\mathbf{x}')=\tilde{A}_q|\mathbf{x}-\mathbf{x}'|^{\tilde{\psi}(q)-D_B} , \tag{2.3}$$

where $D_B=\tilde{\psi}(0)$ is the fractal dimension of the backbone, $[N_{\rm BB}]_{\rm av}\propto|\mathbf{x}-\mathbf{x}'|^{D_B}$, and $\tilde{\psi}(q)$ are the multifractal exponents reviewed in Ref. 1.

The resistance between the two electrodes is given by

$$R(\mathbf{x},\mathbf{x}')=m_1(\mathbf{x},\mathbf{x}') , \tag{2.4}$$

and the corresponding voltage is $V=R$. If, instead of the unit current, we apply a unit voltage between $\mathbf{x}$ and $\mathbf{x}'$, then the resulting currents become $i_b^{(v)}=i_b/R$, and their $2q$th moment is

$$m_q^{(v)}(\mathbf{x},\mathbf{x}')=\sum_b[i_b^{(v)}(\mathbf{x},\mathbf{x}')]^{2q} =m_q(\mathbf{x},\mathbf{x}')/R(\mathbf{x},\mathbf{x}')^{2q} . \tag{2.5}$$

For large $|\mathbf{x}-\mathbf{x}'|$ one expects that one may separate the averages,[15] and therefore[16]

$$M_q^{(v)}=[m_q^{(v)}]_{\rm av}/[N_{\rm BB}]_{\rm av}\propto M_q/[R]_{\rm av}^{2q} . \tag{2.6}$$

Thus, we expect that

$$M_q^{(v)}(\mathbf{x},\mathbf{x}')=\tilde{A}_q^{(v)}|\mathbf{x}-\mathbf{x}'|^{\tilde{\psi}^{(v)}(q)-D_B} , \tag{2.7}$$

with $\tilde{\psi}^{(v)}(q)=\tilde{\psi}(q)-2q\tilde{\psi}(1)$.

Instead of the above averages, we consider here the susceptibility $\chi^{(q)}$ associated with the "correlation function" $m_q^{(v)}(\mathbf{x},\mathbf{x}')$,[4,12]

$$\chi^{(q)}(p)=\sum_{\mathbf{x}'}[m_q^{(v)}(\mathbf{x},\mathbf{x}')]_{\rm av} . \tag{2.8}$$

Since the sum over all $|\mathbf{x}-\mathbf{x}'|$ will effectively be cut off at $|\mathbf{x}-\mathbf{x}'|\sim\xi_p$, we expect that, asymptotically (for $\xi_p\gg 1$)

$$\chi^{(q)}(p)\approx\Gamma_q|t|^{-\gamma-\psi^{(v)}(q)} , \tag{2.9}$$

where $t\equiv p_c-p$, $\psi^{(v)}(q)=\nu\tilde{\psi}^{(v)}(q)$, and $\approx$ means asymptotically equal. Note that $\chi^{(0)}(p)=[N_{\rm BB}]_{\rm av}$.

Following ABH, we next consider the unnormalized moments of $\ln(i_b^{(v)})^2$, defined as

$$\hat{\mu}_k(\mathbf{x},\mathbf{x}')=\sum_b{}'|\ln[i_b^{(v)}(\mathbf{x},\mathbf{x}')]^2|^k , \tag{2.10}$$

where the prime on the summation indicates that the sum is restricted to bonds b for which $0<i_b<1$, and the corresponding susceptibilities

$$\bar{\chi}_k(p)=\left[\sum_{\mathbf{x}:\nu(\mathbf{x},\mathbf{x}')=1}\hat{\mu}_k(\mathbf{x},\mathbf{x}')\right]_{\rm av} , \tag{2.11}$$

where $\nu(\mathbf{x},\mathbf{x}')$ is the indicator function for percolation: $\nu=1$ if $\mathbf{x}$ and $\mathbf{x}'$ are on the same cluster and $\nu=0$ otherwise. Note that $\ln i_b$ is only zero when the bond b connects the two terminals $\mathbf{x}$ and $\mathbf{x}'$. Since these terms are excluded from the sum in Eq. (2.10), we have the relation

$$\chi^{(0)}(p)=dp+\bar{\chi}_0(p) . \tag{2.12}$$

It is easy to convince oneself from Eq. (2.8) that for $k\ge 1$

$$(-1)^k\frac{\partial^k}{\partial q^k}\chi^{(q)}(p)\bigg|_{q=0}=\bar{\chi}_k(p) . \tag{2.13}$$

We next use the normalized susceptibilities, $\chi_k(p)\equiv\bar{\chi}_k(p)/\bar{\chi}_0(p)$, to construct the corresponding cumulants χ_k^c, e.g., $\chi_0(p)=1$ and

$$\begin{aligned}&\chi_1^c=\chi_1=\bar{\chi}_1/\bar{\chi}_0 ,\\ &\chi_2^c=\chi_2-(\chi_1)^2 ,\\ &\chi_3^c=\chi_3-3\chi_2\chi_1+2(\chi_1)^3 ,\end{aligned} \tag{2.14}$$

etc. It is now easy to see that, for positive integer k,

$$\chi_k^c(p)=(-1)^k\frac{\partial^k}{\partial q^k}\ln\chi^{(q)}(p)\bigg|_{q=0} . \tag{2.15}$$

[$\chi^{(q)}(p)$ behaves like the partition function in statistical mechanics.] Using Eq. (2.9), this immediately yields

$$\chi_k^c(p)\approx c_k+d_k\ln|t| \tag{2.16}$$

with

$$c_k=(-1)^k\frac{\partial^k}{\partial q^k}\ln\Gamma_q\bigg|_{q=0} \tag{2.17a}$$

and

$$d_k=(-1)^k\frac{\partial^k}{\partial q^k}\psi^{(v)}(q)\bigg|_{q=0} . \tag{2.17b}$$

Note that c_k and d_k are p independent. Also, c_k, which represents a correction to the leading logarithmic divergence in Eq. (2.16), depends on Γ_q and is therefore nonuniversal, while d_k depends only on $\psi^{(v)}(q)$ and is thus universal. When Eq. (2.14) is inverted we obtain

$$\chi_k=(\chi_1)^k+\frac{k(k-1)}{2}(\chi_1)^{k-2}\chi_2^c+O(|\ln|t||^{k-2}) \tag{2.18a}$$

and use of Eq. (2.16) yields

$$\chi_k=(d_1\ln|t|)^k\left[1+\frac{k}{d_1}\left[c_1+\frac{1}{2}(k-1)\frac{d_2}{d_1}\right]\frac{1}{\ln|t|}+O(|\ln|t||^{-2})\right] \tag{2.18b}$$

in complete analogy with Eq. (3.5) of ABH. We will analyze series expansions for the various logarithmic susceptibilities introduced above, namely, the unnormalized susceptibility $\bar{\chi}_k(p)$ of Eq. (2.11), the normalized susceptibility $\chi_k(p)\equiv\bar{\chi}_k(p)/\bar{\chi}_0(p)$, and the cumulant susceptibility χ_k^c of Eq. (2.14).

As discussed below, we generated series for $\bar{\chi}_k(p)$. Equations (2.13) and (2.18b) imply that

$$\bar{\chi}_k(p)=\bar{\chi}_0(p)\chi_k(p)\approx\Gamma_0|t|^{-\gamma_B}(d_1\ln|t|)^k , \tag{2.19}$$

where $\gamma_B=\gamma+\psi^{(v)}(0)=\gamma+\nu D_B$.

Finally, Eq. (2.18b) may be used to obtain the universal amplitude ratio

$$R_{kl,mn}=\frac{\bar{\chi}_k\bar{\chi}_l}{\bar{\chi}_m\bar{\chi}_n}=1+[k(k-1)+l(l-1)-m(m-1)-n(n-1)]\frac{d_2}{2d_1\ln|t|}+O(|\ln|t||^{-2}) , \tag{2.20}$$

when $k+l=m+n$.

The above derivation of Eq. (2.18b) works only for positive integer k, since it uses the cumulants. However, ABH showed that exactly the same expression also results from a direct integration over the distribution of $\ln i^2$. Taking over their arguments, we expect Eq. (2.18b), and therefore also Eqs. (2.19) and (2.20), to hold for all (positive and negative) k. Note, however, that the expansion in powers of $1/\ln|t|$ becomes inaccurate for large k, when

$$(k/d_1)\left|c_1+\frac{d_2}{2d_1}(k-1)\right|\gtrsim|\ln|t|| .$$

We end this section with some exact theoretical predictions for the behavior of the various susceptibilities at six dimensions, and with some estimates for the coefficients d_k in lower dimensions.

In $d=6-\epsilon$ dimensions Park, Harris, and Lubensky[12] predicted that to leading order in ϵ

$$\psi(q)=1+\frac{a}{(q+1)(q+b)} , \tag{2.21}$$

with $a=\epsilon/14$ and $b=\frac{1}{2}$. Using the ϵ expansion of γ, this is equivalent to

$$\gamma+\psi^{(v)}(q)=2-2q+\epsilon\Theta(q)+O(\epsilon^2) , \tag{2.22}$$

where

$$\Theta(q)=\frac{1}{14(q+1)(q+1/2)}+\frac{3-q}{21} . \tag{2.23}$$

Repeating the renormalization-group solution that led to Eq. (2.21), we note that, in fact, Eq. (2.22) results from the expression

$$\chi^{(q)}(p)\approx|t|^{-2+2q}\left[1+\frac{C}{\epsilon}(|t|^{-\epsilon/2}-1)\right]^{2\Theta(q)} , \tag{2.24}$$

where C is a nonuniversal constant. In the limit $\epsilon\to0$, this yields

$$\chi^{(q)}(p)\propto|t|^{-2+2q}\|\ln|t|\|^{2\Theta(q)} . \tag{2.25}$$

Using Eq. (2.15), we thus find

$$\chi_1^c\approx-2\ln|t|-2\left[\frac{d\Theta}{dq}\bigg|_{q=0}\right]\ln|\ln|t|| \tag{2.26a}$$

$$=-2\ln|t|+\frac{20}{21}\ln|\ln|t|| , \tag{2.26b}$$

and

$$\chi_k^c(p)\approx e_k\ln|\ln|t|| \tag{2.27}$$

for $k\geq2$, with $e_k=(-1)^k2d^k\Theta/dq^k|_{q=0}$. Specifically, $e_2=4$ and $e_3=\frac{180}{7}$.

From Eq. (2.18a) it follows that

$$\chi_k=(\chi_1)^k[1+O(\ln|\ln|t||/(\ln|t|)^2)] . \tag{2.28}$$

We now turn to $d<6$. In $d=6-\epsilon$ dimensions Eqs. (2.21) and (2.17b) yield

$$d_1=2+\tfrac{10}{21}\epsilon+O(\epsilon^2) , \tag{2.29a}$$

$$d_k=\frac{k!}{7}(2^{k+1}-1)\epsilon+O(\epsilon^2) , \quad k\geq2 . \tag{2.29b}$$

Blumenfeld *et al.*[4] used Eq. (2.21) as an approximant for $\psi(q)$ for dimensions $d<6$. Matching with known numerical values of $\psi(0)$ (from D_B), $\psi(1)$ (from the resistance), and $\psi(\infty)=1$, they estimated that $b=1.05\pm0.1$, 0.65 ± 0.08, 0.45 ± 0.1, and 0.33 ± 0.3, and $a=1.22\pm0.01$, 0.40 ± 0.06, 0.15 ± 0.04, and 0.05 ± 0.05 in dimensions 2, 3, 4, and 5, respectively. Substituting into Eq. (2.21), and using Eq. (2.17b), these yield the estimates listed in Table II. Although this approximant gave excellent fits to the

available values of $\psi(q)$, it differs significantly in the derivatives of $\psi(q)$ at $q=0$, especially for the higher orders. We expect the measurements of d_k (such as presented in the present paper) to give guidance on the future construction of better approximants. Since the derivatives d_k are directly related to coefficients in the Taylor expansion of the multifractal function $f(\alpha)$ near its peak,[1] such measurements should also help elucidate the behavior of that function.

III. CONSTRUCTION AND ANALYSIS OF THE SERIES

A. Construction

The method used for constructing the series for $\bar{\chi}_k$ is very similar to that used for $\chi^{(q)}(p)$ in Ref. 4. We define the susceptibilities $\mu_k(\Gamma)$ for a given cluster Γ by

$$\mu_k(\Gamma)=\sum_{\mathbf{x},\mathbf{x}'\in\Gamma}\hat{\mu}_k(\mathbf{x},\mathbf{x}') , \tag{3.1}$$

where $\hat{\mu}_k$ is defined in Eq. (2.10). Calculating the susceptibilities involves averaging over all clusters, and can be written as[17]

$$\bar{\chi}_k(p)=\sum_{\Gamma} W(\Gamma;d)\mu_k^c(\Gamma)p^{n_b(\Gamma)} \tag{3.2}$$

where $n_b(\Gamma)$ is the number of bonds in cluster Γ, $W(\Gamma;d)$ is the number of diagrams per site which are topologically equivalent to Γ in d dimensions (sometimes referred to as the weak embedding constant), and the cumulant susceptibilities $\mu_k^c(\Gamma)$ are defined by

$$\mu_k^c(\Gamma)=\mu_k(\Gamma)-\sum_{\gamma\subset\Gamma}\mu_k^c(\gamma) . \tag{3.3}$$

The summation extends over all subdiagrams γ of Γ, with $\Gamma\neq\gamma$. One should not confuse the cluster cumulant used here with the statistical cumulants χ_k^c of Eqs. (2.14)–(2.16).

Exact results can be obtained for the one-dimensional case, and for the case of the Cayley tree (corresponding to infinite dimension). These will be discussed in Sec. IV. In intermediate dimensions, the sum (3.2) cannot be calculated exactly. The summation involves factors of $p^{n_b(\Gamma)}$ for each cluster Γ of $n_b(\Gamma)$ bonds. Therefore, to calculate the series up to Nth order in p, we need to consider only diagrams with N bonds at most. We calculated the above quantities for $N=13$ and for $-10\le k\le 10$. For each cluster and each pair of terminals $\mathbf{x}$ and $\mathbf{x}'$, we solved Kirchhoff's equations with unit voltage boundary conditions. We then calculated the susceptibilities in the above range of k, in the form

$$\bar{\chi}_k(p)=\sum_{l=1}^{13} a_k(l,m)p^l d^m . \tag{3.4}$$

Up to order p^5, the result is

$$\begin{aligned}\chi_k(p)=&(4d^2-2d)(2\ln 2)^k p^2+(12d^3-12d^2+3d)(2\ln 3)^k p^3+(32d^4-48d^3+16d^2+4d)(2\ln 4)^k p^4\\&+\{(80d^5-160d^4+80d^3+30d^2-25d)(2\ln 5)^k\\&+(4d^3-8d^2+4d)[2(2\ln\tfrac{7}{4})^k+2(2\ln\tfrac{7}{3})^k+6(2\ln 7)^k-3(2\ln 2)^k-4(2\ln 4)^k-6(2\ln 3)^k]\}p^5 .\end{aligned} \tag{3.5}$$

Numerical results up to order p^{13} are available as computer files on request from Adler. In addition to the moment series we have obtained series for the backbone $\chi^{(0)}(p)$ as given by Eq. (2.12); these extend the earlier series[14] by three terms and are explicitly given for dimensions 2–6 in Table I.

Everything stated above can be repeated for unit current boundary conditions, with $\psi(q)$ replacing $\psi^{(v)}(q)$ everywhere. We also constructed series for the corresponding susceptibilities, denoted by $\bar{\chi}'_k(p)$, to $N=11$. These series are also available on request. Note that singly connected bonds do not contribute to $\chi'_k(p)$, hence the corresponding series start from p^4, while $\bar{\chi}_k(p)$ start with p^2.

B. Methods of analysis

We have analyzed the different series by fitting them to several general forms. The first of these has the general form of Eq. (2.19)

$$\bar{\chi}_k\propto(p_c-p)^{-\gamma_k}|\ln(p_c-p)|^{\theta_k} . \tag{3.6}$$

Here we allow θ_k to differ from k and allow γ_k to take different values for each k. We fitted this logarithmic form with the method of Adler and Privman.[6] This analysis involves taking Padé approximants to the series

$$g_k=(-\gamma_k)^{-1}(p_c-p)\ln(p_c-p)\times\left[\left(\frac{\partial\bar{\chi}_k}{\partial p}\Big/\bar{\chi}_k\right)-[\gamma_k/(p_c-p)]\right] . \tag{3.7}$$

The limit of g_k as $p\to p_c$ is θ_k/γ_k. We take Padé approximants to g_k at the exact or most reliable estimate of p_c to obtain graphs of θ_k as a function of γ_k.

The second form replaces the logarithmic factors by nonanalytic confluent corrections,

$$\bar{\chi}_k\approx\Gamma_k(p_c-p)^{-h_k}[1+a_k(p_c-p)^{\Delta_1}+\cdots] , \tag{3.8}$$

TABLE I. Series coefficients, $b(l)$ for the backbone series in dimensions 2–6.

l	$b(l)$	l	$b(l)$
	$d=2$		$d=4$
1	2	7	2 920 900
2	12	8	22 242 992
3	54	9	166 104 180
4	200	10	1 218 312 688
5	686	11	8 821 754 244
6	2 148	12	63 085 682 976
7	6 506	13	447 047 856 400
8	18 520		
9	51 962		$d=5$
10	138 992	1	5
11	370 514	2	90
12	947 200	3	1 215
13	2 436 084	4	14 420
		5	159 665
	$d=3$	6	1 686 030
1	3	7	17 252 795
2	30	8	172 236 520
3	225	9	1 688 750 765
4	1 452	10	16 308 028 890
5	8 691	11	155 652 267 495
6	48 762	12	1 470 375 432 940
7	263 721	13	13 776 257 177 165
8	1 374 408		
9	7 010 619		$d=6$
10	34 882 170	1	6
11	171 153 441	2	132
12	824 671 212	3	2 178
13	3 935 533 761	4	31 704
		5	431 130
	$d=4$	6	5 604 876
1	4	7	70 686 222
2	56	8	871 168 968
3	588	9	10 553 814 894
4	5 392	10	126 080 210 880
5	46 028	11	1 489 660 129 206
6	372 840	12	17 436 318 890 592
		13	202 525 138 659 828

where Γ_k and a_k are nonuniversal amplitudes. This form was used for the backbone series (where we believe it to be correct, with $h_k=\gamma_B$) and for illustrative purposes on some of the other series (where we believe it not to be correct). We fitted this confluent correction form with the methods (M1 and M2) introduced by Adler, Moshe, and Privman,[7,8] and discussed in depth in Ref. 9. In both these methods transformations are made to eliminate the effect of corrections to scaling. In M2, one draws graphs of Padé approximants to the dominant exponent as a function of the trial correction exponent at a trial threshold value. In M1, one draws graphs of Padé approximants to the correction exponent as a function of the trial dominant exponent at a trial threshold value. The predicted set of (γ,Δ_1) values is chosen to be within the region where different approximants give the same results in both methods, and the predicted critical point is that for which optimal convergence is seen. (Note that graphs from both methods are drawn in the same orientation for ease of comparison.)

In order to allow for the possibility of additional correction effects that interfere with our evaluations, we have made the transformation

$$\frac{\ln(p_c-p)}{\ln p_c}=\frac{1}{1-K}\ , \tag{3.9}$$

where, without loss of generality, we may set the critical value of K to be $K_c=1$. This gives an expansion for p, in terms of K: $p=\sum c_n K^n$. The series

$$Y(p)=\frac{\bar{\chi}_k(p)}{dp+\bar{\chi}_0(p)}\approx\frac{(p_c-p)^{-\gamma_B}|\ln(p_c-p)|^k[1+A_k/\ln(p_c-p)+\cdots]}{(p_c-p)^{-\gamma_B}(1+\cdots)} \tag{3.10a}$$

$$\approx[\ln(p_c-p)]^k\left[1+\frac{A_k}{\ln(p_c-p)}\right] \tag{3.10b}$$

is a special case of the more general form

$$Y(p)=|\ln(p_c-p)|^{\theta_k}\left[1+\frac{A_k'}{|\ln(p_c-p)|^{\Delta_x}}+\cdots\right]. \tag{3.11}$$

In both Eqs. (3.10a) and (3.11) the $\cdots$ represent power-law corrections. When the expression from Eq. (3.9) for p in terms of K is substituted into Eq. (3.11), it leads us to a series with the critical behavior

$$Y[p(K)]\sim(K_c-K)^{\theta_k}[1+a_k(K_c-K)^{\Delta_x}+\cdots] \tag{3.12}$$

with $K_c=1$. We have thus transformed the logarithmic corrections into power-law ones. The transformed series can be analyzed by the methods[7-9] discussed above for series with nonanalytic confluent corrections to scaling. This analysis is especially easy since K_c is known. The input value of p_c can be taken from previous analysis of cluster statistics whose accuracy is well established.

In addition to the determination of the critical exponents by the above methods, we have also obtained estimates for the different cumulant amplitudes (d_k and e_k) and universal moment amplitude ratios ($R_{kl,mn}$) defined in Eqs. (2.16), (2.20), (2.26), and (2.27) above. The ratio $R_{kl,mn}$ was evaluated by dividing and multiplying the relevant series and then evaluating Padé approximants to the resulting series at the accurate percolation threshold values of Ref. 9. A similar approach has been used in the past[9] for percolation amplitude ratios, with excellent agreement being achieved with exact and ϵ expansion values.

The cumulant amplitudes d_k were obtained from series for the cumulants by two slightly different approaches which, in principle, should give the same results. In the first approach, d_k [see Eq. (2.16)] was evaluated from the pole-residue plots of Padé approximants to the series for the first derivative of the cumulant series, $\chi_k^c(p)$. (This derivative should have a pole at p_c, with a residue of d_k.) In the second approach, this derivative series was multiplied by (p_c-p) and Padé approximants to the resulting series were evaluated at the p_c values of Ref. 9. The relationship between these two methods is similar to that between the usual D log Padé and threshold biased D log Padé methods. The amplitudes e_k for $k\geq 2$ in six dimensions [see Eq. (2.27)] were evaluated in the spirit of the latter approach only; the derivatives of the cumulant series were multiplied by $(p_c-p)\ln(p_c-p)$ to give a series to which Padé approximants were evaluated at p_c. The first cumulant in six dimensions, eqs. (2.26b), was studied in a similar manner.

The straightforward methods used for the amplitudes do not explicitly allow for further corrections to scaling. In theory such corrections should be taken into account, however, it is questionable if the relatively short series contain enough information to make this worthwhile in practice.

IV. RESULTS IN ONE DIMENSION AND ON CAYLEY TREES

A. Exact results

In one dimension the sum in Eq. (3.2) can be calculated exactly. The easiest way to evaluate this sum is to return to $\chi^{(q)}(p)$, Eq. (2.8). The cluster cumulant of $m_q^{(v)}$ for a chain of n bonds is simply n^{1-2q} [the current between the end points is $i^{(v)}=1/n$, and all other pairs $(\mathbf{x},\mathbf{x}')$ cancel after the cumulant subtraction]. Also $W=1$. Thus,

$$\chi^{(q)}(p)=\sum_{n=1}^{\infty}n^{1-2q}p^n\,. \tag{4.1}$$

Starting with the geometric sum, it is easy to check that for every integer $2q\leq 1$, one has

$$\chi^{(q)}(p)=\frac{\Gamma(2-2q)}{(1-p)^{2-2q}}[1+O(1-p)]\,, \tag{4.2}$$

where $\Gamma(x)$ is the gamma (factorial) function. Thus, $\psi^{(v)}$ has a constant gap exponent equal to $2\psi(1)=2$, and the distribution is not multifractal. The same result is also found for all real $2q\leq 1$, if one replaces the sum (4.1) by an integral. The difference between the sum and the integral is of order $(1-p)^0$, and is therefore negligible to the leading order in Eq. (4.2). Using Eq. (4.2) for q near zero now yields

$$\chi_k^c=(-1)^k\frac{\partial^k}{\partial q^k}\ln\Gamma(2-2q)\bigg|_{q=0}$$
$$-2\delta_{k,1}\ln(1-p)+O(1-p)\,, \tag{4.3}$$

i.e.,

$$\chi_1=\chi_1^c\approx 2[\Psi(2)-\ln(1-p)]$$
$$\approx 2[0.422\,784\,335-\ln(1-p)]\,, \tag{4.4}$$

$$\chi_k^c\approx 2^k\frac{\partial^{k-1}}{\partial x^{k-1}}\Psi(x)\bigg|_{x=2}$$
$$=(-2)^k(k-1)![\zeta(k)-1]\,,\quad k\geq 2\,, \tag{4.5}$$

where $\Psi(x)$ is the digamma function and $\zeta(k)$ is Riemann's ζ function. Since there is no multifractality in $\chi^{(q)}$, all the cumulants χ_k^c (except the first) are numbers, associated with derivatives of the *amplitude* in $\chi^{(q)}$.

Using Eqs. (2.18a) and (4.4) we now see that

$$\bar{\chi}_k = \chi^{(0)}\chi_k \approx |2\ln(1-p)|^k/(1-p)^2 \ . \tag{4.6}$$

For the Cayley tree, one replaces p^n in Eq. (4.1) by $[z/(2\sigma)](p\sigma)^n$, where $\sigma = z-1$ and z is the coordination number. Thus, Eqs. (4.4)–(4.6) are still valid, but with p replaced by $p\sigma$, i.e., $p_c = 1/\sigma$. These should represent the leading behaviors for dimension $d > 6$. Note, however, that at any finite d, one has exponentially small currents[1,4] that may modify the behavior of $\chi^{(q)}$ for some $q < 0$ and affect the leading behavior of χ_k for very large $|k|$. For the unit current boundary conditions, $i_b \equiv 1$ and $\chi'_k \equiv 0$, for any such structure in which no loops are permitted.

B. Series analysis in one dimension

Although we know the exact result for $d = 1$, it is instructive to analyze the series expanded to any desired order from the exact expressions. Since $i^{(v)} = 1/n$, Eqs. (3.1)–(3.3) yield $\mu_k^c = n(\ln n^2)^k$, and therefore $\bar{\chi}_k(p) = \sum_{n=1}^{\infty} n(\ln n^2)^k p^n$. (We note that series derived from this definition agree perfectly with one-dimensional series calculated from the general formalism, as expected.)

Unless explicitly noted, all results are given for $\bar{\chi}_k$, which should behave as in Eq. (4.6). A typical result from the method explained just after Eq. (3.6) for $k = -2$ is shown in Fig. 1(a), for a series with 20 terms. We have analyzed $\bar{\chi}_k/p^2$, since the first two terms in the expansion are zero, and plotted θ_k versus γ_k. The exact form gives $\gamma_k = \gamma_{-2} = 2$ and $\theta_k = k = \theta_{-2} = -2$. We see that all the Padés in the figure (we have selected diagonal and near diagonal ones) pass through the point $(\gamma_{-2} = 2, \theta_{-2} = -2)$ as expected. Similar quality of convergence is found for 20 terms for $-4 < k < 6$. However, for larger positive k values there is a general downgrading of quality of convergence. For $k \le -4$ we find that the approximants to θ_k as a function of γ_k do not converge to the correct value of $(\gamma_k = 2, \theta_k = k)$ and pass instead through the origin, indicating the wrong "result" $\gamma_k = \theta_k = 0$. This implies that the series in question do not appear to have the expected singularity at $p = 1.0$. An example of this behavior for $k = -6$ is given in Fig. 1(b).

In Fig. 2, we plot estimates of γ_k [Eq. (3.6)] or h_k [Eq. (3.8)] versus k from several different analyses of the 20-term series. The results for γ_k are indicated by the solid circle symbol. Above $k = -3$ we obtained the expected exact value $\gamma_k = 2$. However, there is an apparent crossover near $k = -4$ to an absence of singularity. Since we know that there is no real crossover from $\gamma_k = 2$ to 0 in one dimension, we conclude that this is a numerical problem for this method of analysis caused by shortness of the series. To test this we extended the series further. The series for $k = -4$ and -5 indeed gave the expected convergence to $\gamma_k = 2$ for some 25–28 terms. Although it is quite easy to generate longer series to extend this test to even higher k values, it is somewhat inconvenient to carry out the logarithmic analysis for series over 30 terms, and the improvement as we extended the series for $k > -5$ was rather slow. Thus, instead of trying to determine whether we can obtain a singularity for, say, $k = -6$ for the longer series, we investigated the effect of reducing the length of the series with smaller $|k|$ values. In fact, we are actually more interested in the behavior of the shorter series in order to help analyze the series in higher dimensions. We carried out the analysis for different lengths for $k = -3$ and illustrate the results for 23 terms and 11 terms in Figs. 1(c) and 1(d). We see that the 23-term series passes through the point $(\gamma_{-3} = 2, \theta_{-3} = -3)$ as it should, but the 11-term series fails to pass through that point. We conclude that the apparent absence of a singularity for the lower negative moments is an artifact of the (relative) shortness of the series.

At $k = 0$ there is no logarithmic correction, and therefore Eq. (3.8) is the correct form. Indeed, in this case we fitted the series to Eq. (3.8) and observed the expected $\gamma = \gamma_B = 2$. Furthermore, we found that the graph of γ as a function of Δ_1 for this case (not shown) is a perfect example of confluent correction analysis for a series with only analytic ($\Delta_1 = 1.0$) corrections to scaling and resonances at $\Delta_1 = \frac{1}{2}$ and $\frac{1}{3}$ (Ref. 11) for 11 terms. For 20 terms the resonances disappear, in a similar manner to that described in Appendix D of Ref. 11.

We have also attempted to fit the one-dimensional series for $k \neq 0$ with Eq. (3.8). This is obviously not the correct form for these series since we have just shown that their exact form includes a logarithmic correction. However, we wanted to see what results we would obtain without being biased by the theoretical predictions. The results of this analysis are presented as h_k in Fig. 2. Series of both 11 (indicated by $\times$) and 20 (indicated by $+$) terms have been analyzed. Results are given either for best convergence or for $\Delta_1 = 1.0$, with very little discrepancy between the two criteria in any case. We see that there is a somewhat better convergence for the 20-term series, although we do not obtain the expected $h_k = 2$ for any $k \neq 0$. There were no signs of any intersection region which would indicate a strong nonanalytic confluent correction to scaling.

Looking at the estimates of h_k at $\Delta_1 = 1.0$ (presented in Fig. 2) it is rather amazing how strongly these effective exponent values deviate from two when the logarithmic correction is not allowed for. These results show that the power-law correction of Eq. (3.8) does a bad job of mimicking the correct logarithmic form of Eq. (3.6). These h_k estimates are clearly contrary to our expectation that $h_k \equiv 2$ for all k. However, they are of some interest because they show that if we were to analyze the one-dimensional moments of the current logarithms without suspecting logarithmic corrections, we might conclude that instead of having a constant γ_k we had k-dependent values with a gap. (Looking at the h_k values for $k > 0$ gives the impression that while this gap seems k independent for the 20-term series, it seems to increase with k for the 11-term series. From the exact form we know that for a long enough series h_k should be constant, and therefore that we should expect a decrease in all h_k towards the correct constant value as the series length increases.) The apparent observed gap reflects the fact that this

analysis mimics the correction $|\ln(1-p)|^k$ as $(1-p)^{kx}$, with a small x (which should decrease as the series lengthens.) It is clear from the above that the way to exclude such apparent behavior, with a gap, is by studying the dependence of the behavior on the series length. When the deviations are spurious they will become less marked as the series length increases. It should be noted that for this case the number of terms needed to actually obtain a constant h_k was more than the maximum (30). Another moral of this is that it is helpful to have theoretical guidance for the expected singular form.

V. RESULTS IN HIGHER DIMENSIONS

A. Backbone exponents

There is one additional matter of concern that requires attention before we can discuss our results for the moments. This is the question of the determination of γ_k for the case of $k=0$. We shall call this exponent γ_B because it is the same exponent as the backbone susceptibility exponent. The backbone susceptibility exponent is related to the backbone fractal dimension, D_B, via the scaling relation $D_B=(\gamma_B-\gamma)/\nu$. For two and three dimensions, Herrmann and Stanley found from simulations[13] $D_B=1.62\pm0.02$ and 1.74 ± 0.04, respectively. These imply (using exact exponents in two dimensions and $\gamma=1.8$ and $\nu=0.88$ in three dimensions) $\gamma_B=4.54\pm0.02$ ($d=2$) and $\gamma_B=3.33\pm0.10$ ($d=3$). The tenth-order series estimates of Hong and Stanley[14] lead to $\gamma_B=4.79\pm0.05$ ($d=2$) and $\gamma_B=3.41\pm0.07$ ($d=3$).

We have made our own determination from our backbone susceptibility series (see Table I). This determination has been made using the confluent form [Eq. (3.8)], as we have no reason to suspect logarithmic corrections

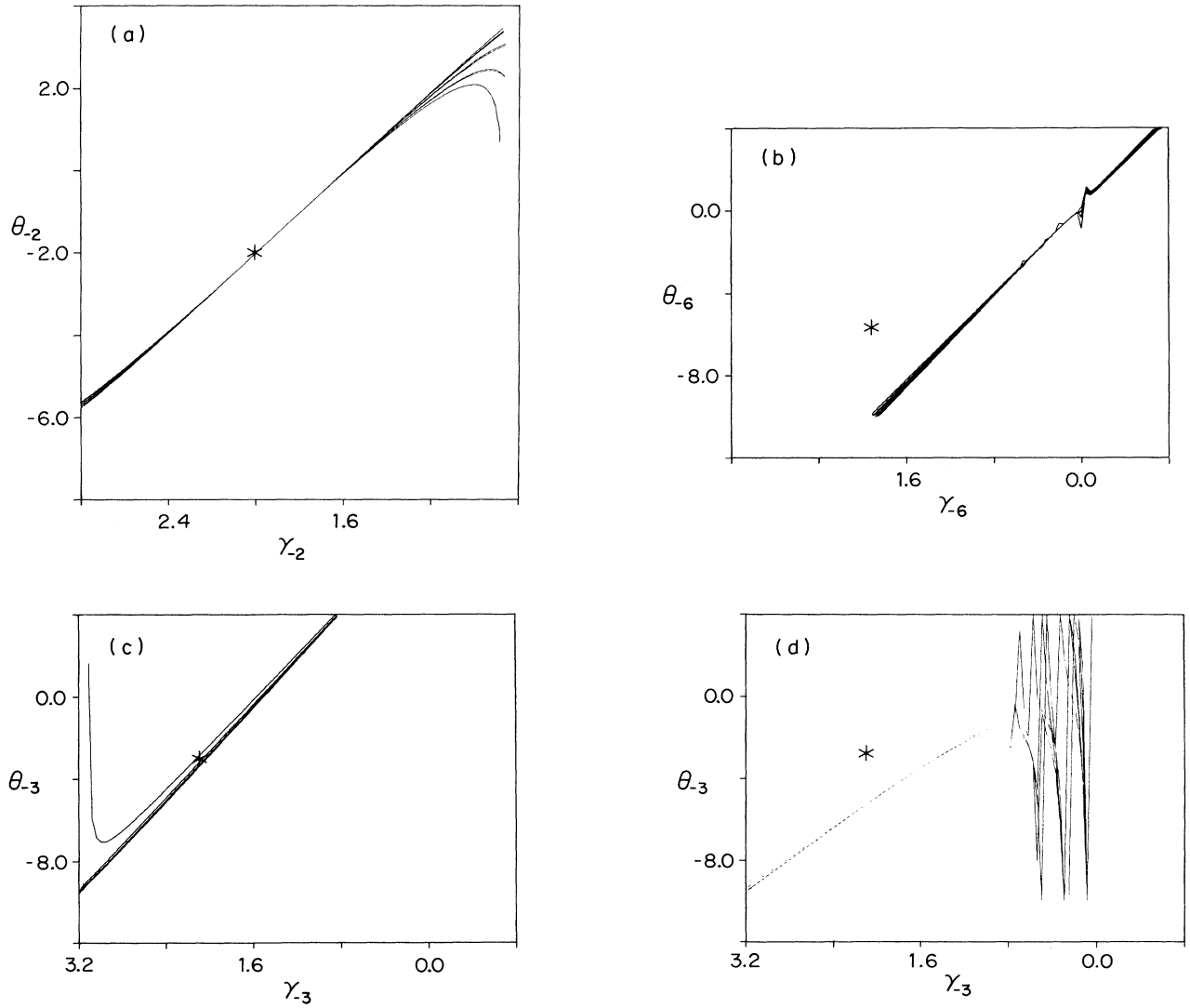

FIG. 1. Graphs of Padé approximants to θ_k as a function of γ_k for the one-dimensional moments $\bar{\chi}/p^2$ for (a) 20 terms; $k=-2$, (b) 20 terms; $k=-6$, (c) 23 terms; $k=-3$, (d) 11 terms, $k=-3$. The exact results are indicated by asterisks.

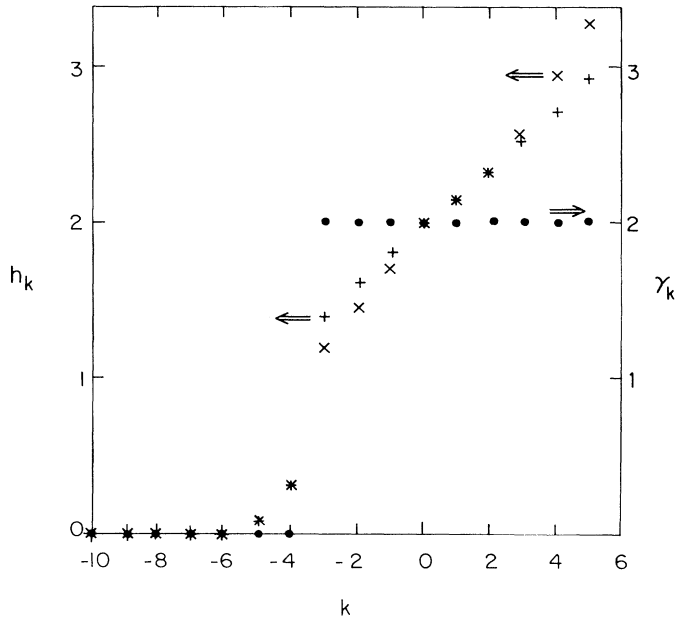

FIG. 2. Graph of γ_k and h_k estimates as a function of k for one-dimensional 20- and 11-term series. γ_k are indicted by ● (20 terms) and h_k are indicated by + (20 terms) and × (11 terms). The points indicated by ● have $\theta_k = k$ and the others have $\theta_k = 0$ and $\Delta_1 = 1.0$ except for $k = -4$ where $\Delta_1 > 1.0$. The exact result is $\gamma_k = 2.0$ for all k.

at $k = 0$. We find from this analysis at the best Δ_1 convergence

$$\gamma_B = 4.45 \pm 0.08 \ , \quad \Delta_1 = 1.7 \pm 0.3 \ , \quad d = 2 \ , \quad p_c = 0.5 \ ,$$

$$\gamma_B = 3.52 \pm 0.08 \ , \quad \Delta_1 = 1.2 \pm 0.2 \ , \quad d = 3 \ , \quad p_c = 0.2492 \ ,$$

and

$$\gamma_B = 3.45 \pm 0.08 \ , \quad \Delta_1 = 1.0 \pm 0.2 \ , \quad d = 3 \ , \quad p_c = 0.2486 \ .$$

The three-dimensional results have essentially the same correction exponent, of order 1.1 ± 0.3, as the usual percolation susceptibility[18] but the two-dimensional value is higher. If we assume that the backbone susceptibility should have the same leading correction exponent as the usual percolation susceptibility[19] then for $d = 2$ we would have $\Delta_1 = 1.25 \pm 0.15$,[18] which gives $\gamma_B = 4.55 \pm 0.10$. We see that this γ_B value is in excellent agreement with the Monte Carlo result of Ref. 13 but does not agree so well with the series result of Ref. 14 where allowance was not made for corrections to scaling. The agreement with Monte Carlo simulations suggests that the correction exponent may be the same as the usual one, as might be expected theoretically.[19] Our three-dimensional result is a weak function of the p_c choice, and at the currently accepted[9] $p_c = 0.2488$ we have $\gamma_B = 3.48 \pm 0.08$ and $\Delta_1 = 1.1 \pm 0.2$. Throughout the convergence range the three-dimensional value is higher than both the previous recent evaluations. Both our values do agree, however, with the older Monte Carlo simulations of Kirkpatrick,[20] who found $\gamma_B = 3.38$–3.64 ($d = 3$) and $\gamma_B = 4.45$–4.55 ($d = 2$). Illustration of these evaluations can be found in Figs. 3(a) and 3(b), where we present graphs from M2 in $d = 2$ and M1 in $d = 3$, respectively. We surround the region where the different Padé approximants appear to best converge with boxes and illustrate the two-dimensional Δ_1 value from the usual susceptibility series with an asterisk. For each dimension we chose to display that method which gave the clearest convergence, but note that in each case the other method gives compatible results. We see that the series value of Ref. 14 for two dimensions corresponds to $\Delta_1 = 1.0$, as expected from the lack of allowance for corrections there. These series are very short for reliable determination of correction values, although we would hope that they are long enough to determine dominant exponents reliably.

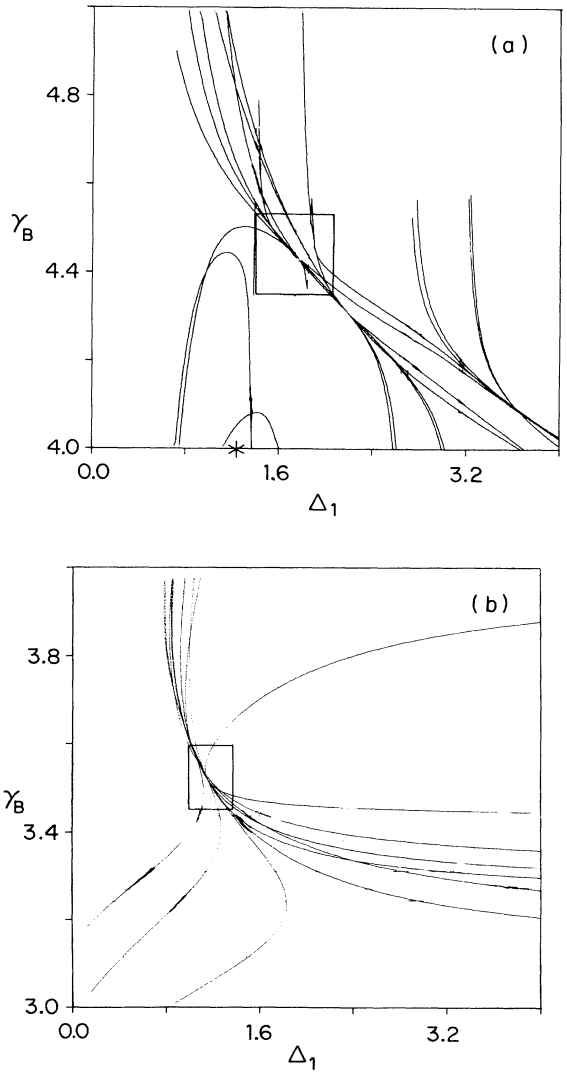

FIG. 3. Graphs of Padé approximants to γ_B as a function of Δ_1 for the backbone series with (a) two dimensions using M2 and (b) three dimensions using M1.

B. Critical exponents for $k \neq 0$

Let us now consider the series in two and three dimensions, for $k \neq 0$. In view of the potential ambiguities we encountered in our unbiased analysis of the one-dimensional series, it is helpful to recall the general theory presented in Sec. II. There it is entirely clear [see Eq. (2.19)] that $\gamma_k = \gamma_B$. We therefore used Eq. (3.6) with $\gamma_k = \gamma_B$ to determine θ_k from the series. As described below Eq. (3.7) in Sec. III B, the determination was made by generating graphs of Padé approximants to θ_k as a function of trial γ_k, and then reading off the value of θ_k at our accurately determined values of γ_B. (In addition to the analysis for $\gamma_k = \gamma_B$, we began, but have not explicitly summarized, an analysis based on the possibility that $\gamma_k \neq \gamma_B$ with some $\theta_k \neq 0$. These calculations failed to converge to any consistent exponent values.)

We present typical graphs of our results in Fig. 4(a) for θ_2 in $d = 2$ and in Figs. 4(b) and 4(c) for θ_1 and θ_3, respectively, in $d = 3$. A summary of our estimates for θ_k for general $k > 0$ is given in Fig. 5, where it can be seen that for $0 \leq k \leq 6$ in $d = 2$ and for $0 \leq k \leq 3$ in $d = 3$, $\theta_k \approx k$. For larger k values there is a systematic deviation with θ_k being a little larger than the predicted (2.19) value of k. Results of the analysis for $k = -1$ and -2 gave $\theta_k = k$ with similar quality of convergence as that in Fig. 4. However, below $k = -3$ the situation is not so clearcut. As in one dimension, our series again suggest that $\gamma_k \to 0$ as k decreases below $k = -3$. In one dimension the exact form told us that this was spurious. In higher dimensions we cannot at present propose any numerical method to further investigate this problem based on the series at hand at this time. We conclude that our numerical results show that there is the same qualitative behavior in two and three dimensions as in one dimension. Wherever the series are not too short we see agreement with the theoretical predictions.

It is also of interest to summarize the results obtained

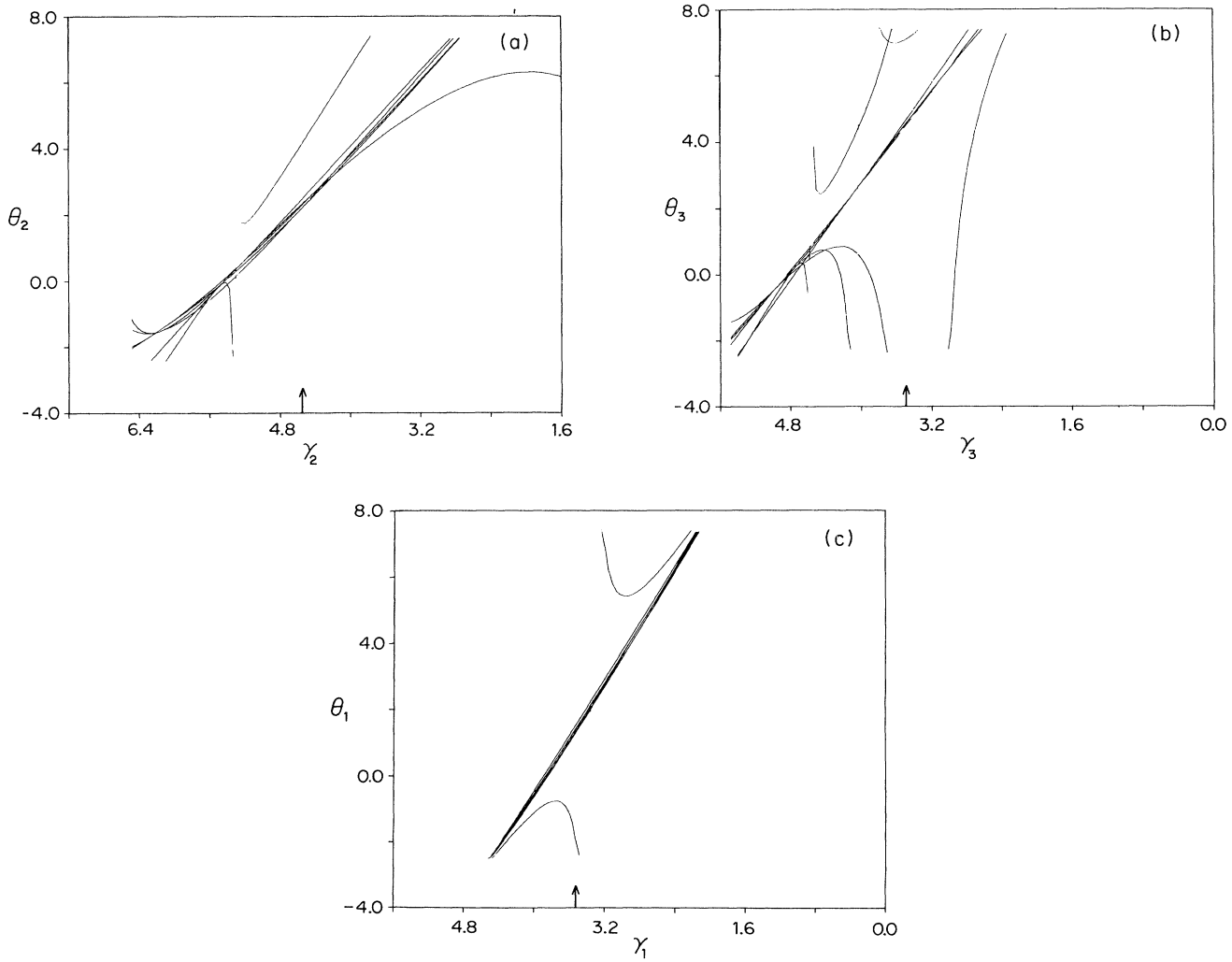

FIG. 4. Graphs of Padé approximants to θ_k as a function of γ_k for 11 terms for $\bar{\chi}_k/p^2$ with (a) $k = 2$, two dimensions, (b) $k = 3$, three dimensions, and (c) $k = 1$, three dimensions. The exact $\gamma_k = \gamma_B$ are indicated by arrows.

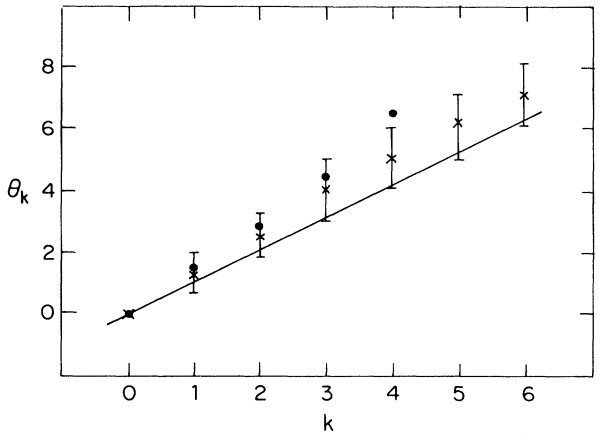

FIG. 5. Graph of θ_k estimates as a function of k for the two- and three-dimensional $\bar{\chi}/p^2$ series, indicated by ● and ×, respectively. The error bars are composites of the errors in θ and in γ_B and are explicitly given for the two dimensional values. The three dimensional errors have similar magnitude but are centered on the three-dimensional θ_k values. θ_k for $\partial^2\bar{\chi}/\partial p^2$ are very close to these values. The line $\theta_k = k$ is drawn for comparison.

from fitting to Eq. (3.8), which we believe to be incorrect. We studied several series, including $\partial^2\bar{\chi}_k/\partial p^2$, $(\partial\bar{\chi}_k/\partial p)/p$, and $\bar{\chi}_k/p^2$, with both M1 and M2. We again found that for positive k there is an apparent variation of h_k as a function of k. This is strongest for $\partial^2\bar{\chi}_k/\partial p^2$ in two dimensions and weakest for $\bar{\chi}_k/p^2$ in three dimensions. The error bars are extremely large here, and the curvature varies for different derivatives.

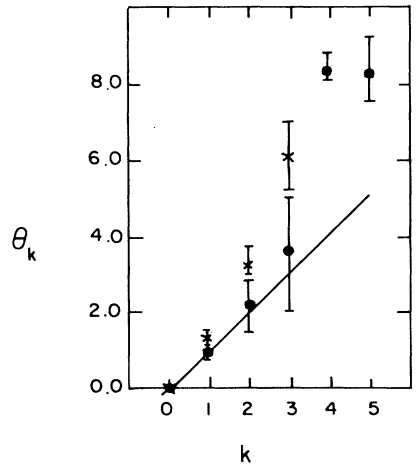

FIG. 6. Graph of θ_k estimates as a function of k for the two- and three-dimensional $\bar{\chi}'/p^2$ series, indicated by ● and ×, respectively. The error bars are composites of the errors in θ and in γ_B and are explicitly given for the two-dimensional values. The three-dimensional errors have similar magnitude but are centered on the three-dimensional θ_k values. θ_k for $\partial^2\bar{\chi}/\partial p^2$ are very close to these values. The line $\theta_k = k$ is drawn for comparison.

Accordingly, and in view of the theory, (which gives $h_k = \gamma_B$), we discard this analysis.

The analyses of the previous subsections confirm behavior of the type of Eq. (3.6), but for larger k, θ_k does not appear to be exactly k for $d > 1$. One possible explanation is that higher-order corrections interfere with the analysis for the larger values of k. In order to remove one possible type of interfering corrections [those described in Eq. (3.10)] we have made the transformations (3.9) discussed above. The transformed series indeed gave poles at the expected $K_c = 1$ with the expected analytic correction to scaling. However, we again obtained slight deviations from the exact $\theta_k = k$. (For θ_1 we quote 1.2 ± 0.3, and conclude that while for small k, $\theta_k \approx k$, this does not seem to be true for $k \geq 3$.) These deviations indicate that our series appear to have some additional complications that lead to effective corrections to the (relatively) short series. We note[18] that our methods M1 and M2 provide no improvement over a simple (threshold biased) D log Padé method when the corrections are analytic as in this case. Thus, our analysis of the series in K did confirm the nontrivial prediction that $\Delta_x = 1$, but yielded no improvement on the estimates of θ_k.

In addition to $\bar{\chi}_k$ we have also analyzed $\bar{\chi}'_k(p)$, calculated for the unit current boundary condition. A graph of θ_k versus k is given in Fig. 6 for positive k (negative k failed to converge). Results are similar to those for $\bar{\chi}_k$.

C. Critical amplitudes

In order to determine conclusively whether the form of Eq. (2.19) can be observed in the finite series, we turned to the evaluation of the cumulant amplitudes d_k with the techniques described above. If the series yield estimates of d_k, which are in general agreement with those from the approximants cited in Table II, then we will gain confidence that the behavior of Eq. (2.16) holds and that correction terms are interfering with the exponent

TABLE II. Results for the cumulant amplitudes, d_k, Eq. (2.17b). The approximant is based on Eq. (2.21), with the values for the constants a and b being given in the text following Eq. (2.29).

d	Series	Approximant
	First cumulant	
2	5.0±1.0	4.9
3	3.4±0.4	3.8
4	3.0±0.10	3.2
5	2.48±0.08	2.7
	Second cumulant	
2	8.0±2.0	6.6
3	4.0±0.2	6.0
4	1.8±0.4	5.4
5	0.8±0.2	4.0
	Third cumulant	
2	16.0±4.0	26.0
3	3.2±.08	32.0
4	0.4±0.16	38.0
5	≈0	37.0

analysis. If the d_k estimates are of a high quality, and if they disagree with the approximant in Table II, then we will have a very nice bonus because, as noted above, there is independent motivation for accurate evaluation of d_k in order to improve the quality of approximants of the type discussed in Ref. 4.

For the first approach to the amplitude analysis (see end of Sec. III B) in $d<6$, we obtained the results given in the first column of Table II. A sample pole-residue plot is given in Fig. 7 for the case of the second cumulant in $d=4$. The second approach gave similar results, with good consistency between different Padé approximants. In the second approach we did not find a strong dependence on threshold choice within the range of thresholds given in Ref. 9.

In order to compare the series for the first cumulant in six dimensions with the predicted equation (2.26b) it was necessary to subtract the additional $-2\ln|p_c-p|$ contribution. This subtraction led to a series whose amplitude was strongly threshold dependent and in comparison with the exact $e_1=\frac{20}{21}$, we quote 0.9 at $p_c=0.0940$ and 1.26 at $p_c=0.0942$ from the [5,5] Padé approximant and consistent values for other high central approximants. (The $[m,n]$ Padé approximant is the ratio of polynomials of degrees m and n that are used to approximate a power series. It is believed[21] that that highest central and nearest diagonal approximants provide the best approximation for the series. [5,5] is the highest central approximant for our cumulant series.) For e_k of the higher cumulants, we did not observe a strong p_c dependence. However, there is considerable scatter between different approximants. For e_2 the [5,5] approximant gives 2.3 at $p_c=0.0942$ whereas others such as [4,4] give 3.8 in far better agreement with the exact $e_2=4$. For the third cumulant convergence is very poor.

The universal amplitude ratios $R_{kl,mn}$ have been evaluated for several cases. Equation (2.20) predicts that $R_{kl,mn}=1+f(kl,mn)\delta$, where

$$f(kl,mn)\equiv[k(k-1)+l(l-1)-m(m-1)-n(n-1)]$$

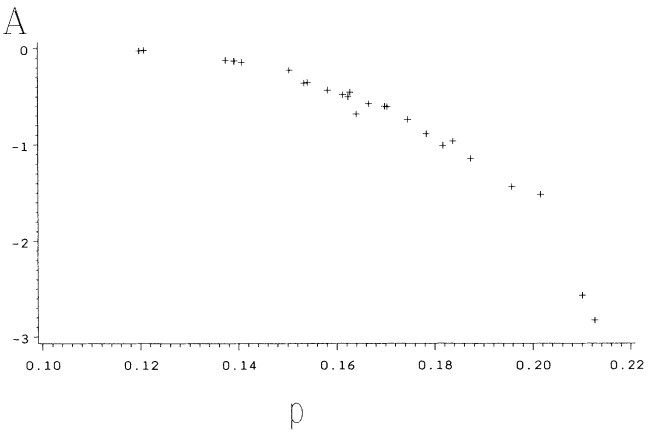

FIG. 7. Pole-residue plot of an amplitude as a function of threshold for the second cumulant in four dimensions.

and where $\delta=d_2/(2d_1\ln|p_c-p|)$ is p dependent but should be independent of k, l, m, and n. Very close to p_c, δ should be extremely small, and we expect that $R_{kl,mn}$ will be close to unity. We calculated Padé approximants for the ratios $R_{kl,mn}$ at the most accurate available values of p_c, i.e., those estimated from 15-term series for $d>2$ in Ref. 9 and also at the exact $p_c=\frac{1}{2}$ for $d=2$.

The measured values of $R_{kl,mn}$ were indeed close to unity in all dimensions below 6, but were not exactly equal to unity. We interpret the small differences as resulting from the fact that our 13-term series would yield effective thresholds which are somewhat different from the values we actually used. Assuming $R_{kl,mn}=1+f(kl,mn)\delta$, we estimated δ. In two dimensions, we made two different evaluations of δ, averaging separately over cases of $|f(kl,mn)|=2$ and $|f(kl,mn)|=8$. For each (kl,mn) set we averaged over four of the five highest approximants (thereby discarding several approximants that are extremely different from the average) to find central average values of $\delta=0.048$ for $|f(kl,mn)|=2$ and $\delta=0.043$ for $|f(kl,mn)|=8$. As usual in Padé analysis, errors are difficult to determine, but all the approximants that are not extremely different fall within some 10% of the average values cited above. In $d>2$, δ is small, but it has larger scatter than for $d=2$. This analysis shows that the finite series estimates do behave according to the prediction of Eq. (2.20), thereby confirming that Eq. (2.19) correctly describes the moments.

VI. DISCUSSION AND CONCLUSION

We have described the transformation of the results of ABH into a form suitable for comparison with low concentration series and generated series for moments of the distribution of the logarithms of the currents in percolating resistor networks. Extensive detailed predictions for the behavior of the moments and of cumulants and ratios derived therefrom have been given and compared with series for moments, cumulants and ratios.

From this project we reach the following conclusions.

(1) We extended the series for the percolation backbone by three terms in general dimension. In two and three dimensions our new $\gamma_B=4.55\pm0.10$ and 3.48 ± 0.08 give fractal dimensions $D_B=1.62\pm0.08$ and 1.91 ± 0.15, respectively. The two-dimensional results are in excellent agreement with the simulations of Refs. 13 and 20, but not with the shorter series of Ref. 14. In three dimensions our backbone exponent and fractal dimension are higher than those of both Refs. 13 and 14, and in agreement with Ref. 20.

(2) By comparing our series analysis to exact results in one dimension, we were able to assess the validity of various analysis procedures. The main conclusion was that knowing the correct asymptotic form to which to fit was very important.

(3) We analyzed series for the moments of the distribution of the logarithms of the currents $\bar{\chi}_k(p)$ as defined in Eq. (2.11), according to the behavior

$$\bar{\chi}_k(p) \propto (p_c - p)^{\gamma_B} |\ln(p_c - p)|^{\theta_k} .$$

Our results, shown in Fig. 5, are consistent with the theoretical prediction $\theta_k = k$.

(4) We attempted to determine the amplitudes, d_k, in the cumulant susceptibility $\chi_k^c(p)$ discussed in Eqs. (2.15) and (2.16). Because the d_k's are proportional to the kth derivative of the "noise" exponent $\tilde{\psi}(q)$, they are universal. For $k = 1$ and 2 our series determinations are more accurate than existing simple approximants to $\tilde{\psi}(q)$.

(5) We also studied amplitude ratios, $R_{kl,mn}$, defined in Eq. (2.20), which are expected to be universal. Our results, given in Sec. V B, are consistent with the theoretical prediction $\lim_{p \to p_c} R_{kl,mn} = 1$.

ACKNOWLEDGEMENTS

We thank the US–Israel Binational Science Foundation and the Israel Academy of Science and Humanities for support. R.B. acknowledges partial support from the Science and Engineering Research Council, U.K. A.B.H. acknowledges support from the MRL program of the U.S. NSF under Grant. No. DMR-88-15469.

*Permanent address: Department of Physics, Technion, Haifa, 32000, Israel; electronic address: phr76ja@technion.technion.ac.il
†Electronic address: c21@ve.tau.ac.il
‡Present address: Princeton Materials Institute, E304 Engineering Quadrangle, Princeton University, Princeton, NJ 08544-5263; electronic address: rafi@matter.princeton.edu
§Electronic address: harris@mohlsun.physics.upenn.edu
**Present address: Department of Physics, University of California, Santa Barbara, CA 93106.

[1]A. Aharony, R. Blumenfeld, and A. B. Harris, preceding paper, Phys. Rev. B **47**, 5756 (1993).
[2]E. Duering and D. J. Bergman, J. Stat. Phys. **60**, 363 (1990); E. Duering, R. Blumenfeld, D. J. Bergman, A. Aharony, and M. Murat, *ibid.* **67**, 113 (1992).
[3]For a recent review, see J. Adler, Y. Meir, A. Aharony, A. B. Harris, and L. Klein, J. Stat. Phys. **58**, 511 (1990).
[4]R. Blumenfeld, Y. Meir, A. Aharony, and A. B. Harris, Phys. Rev. B **35**, 3524 (1987).
[5]D. Stauffer and A. Aharony, *Introduction to Percolation Theory* (Taylor and Francis, London, 1992).
[6]J. Adler and V. Privman, J. Phys. A **14**, L463 (1981).
[7]J. Adler, M. Moshe, and V. Privman, Phys. Rev. B **26**, 1411 (1982).
[8]J. Adler, M. Moshe, and V. Privman, J. Phys. A **14**, L363 (1981).
[9]J. Adler, Y. Meir, A. Aharony, and A. B. Harris, Phys. Rev. B **41**, 9183 (1990).
[10]See, e.g., D. L. Hunter and G. A. Baker, Jr., Phys. Rev. B **7**, 3346 (1973); Y. Meir, J. Phys. A **20**, L349 (1987).
[11]L. Klein, J. Adler, A. Aharony, A. B. Harris, and Y. Meir, Phys. Rev. B **43**, 11 249 (1991).
[12]Y. Park, A. B. Harris, and T. C. Lubensky, Phys. Rev. B **35**, 5048 (1987).
[13]H. Herrmann and H. E. Stanley, Phys. Rev. Lett. **53**, 1121 (1984); H. Herrmann, H. E. Stanley, and D. C. Hong, Phys. Rev. A **17**, L261 (1984).
[14]D. C. Hong and H. E. Stanley, J. Phys. A **16**, L475 (1983).
[15]A. B. Harris and T. C. Lubensky, Phys. Rev. B **35**, 6964 (1987).
[16]L. deArcangelis, S. Redner, and A. Coniglio, Phys. Rev. B **34**, 4656 (1986).
[17]R. Fisch and A. B. Harris, Phys. Rev. B **18**, 416 (1978).
[18]J. Adler, M. Moshe, and V. Privman, in *Percolation Structures and Processes*, edited by G. Deutscher, R. Zallen, and J. Adler, Annals of the Israel Physical Society Vol. 5 (Adam Hilger, Bristol, 1983), p. 397.
[19]This is indeed the case in $6-\epsilon$ dimensions.
[20]S. Kirkpatrick, in *Electrical Transport and Optical Properties of Inhomogeneous Media (Ohio State University, 1977)*, Proceedings of the First Conference on the Electrical Transport and Optical Properties of Inhomogeneous Media, AIP Conf. Proc. No. 40, edited by J. C. Garland and D. B. Tanner (AIP, New York, 1978), p. 99.
[21]D. S. Gaunt and A. J. Guttman, in *Phase Transitions and Critical Phenomena*, edited by C. Domb and M. S. Green (Academic, New York, 1974), Vol. 3.